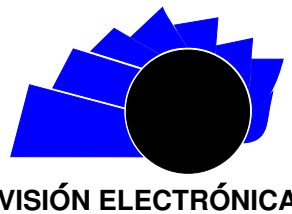




# Visión Electrónica

## Más que un estado sólido

<https://revistas.udistrital.edu.co/index.php/visele>



A RESEARCH VISION

## Distribution system with wind penetration

### Sistema de distribución con penetración eólica

Ernesto Jair Eguis-Eslava <sup>1</sup>, Kelly Marcela Padilla-García <sup>2</sup>, Luis Alberto López-Díaz <sup>3</sup>, José Daniel Soto-Ortiz <sup>4</sup>, Rafael Castillo-Sierra <sup>5</sup>, Mauricio Pardo-González <sup>6</sup>, Cesar Augusto Orozco-Henao <sup>7</sup>, Elvin Arnaldo Jiménez-Matos <sup>8</sup>, Ingrid Oliveros-Pantoja <sup>9</sup>

#### INFORMACIÓN DEL ARTÍCULO

##### Historia del artículo:

Enviado: 10/09/2018

Recibido: 27/09/2018

Aceptado: 25/10/2018

##### Keywords:

Distributed Generation

Electrical Losses

Energy Efficiency

IEEE-13

Renewable Energies

Wind energy

#### ABSTRACT

This article presents analysis of the operation results of a modified IEEE-13 distribution feeder, which was built to scale in the laboratory at the Universidad del Norte. In this article, we show the operating regime cases of the modified IEEE-13, under different levels of wind energy penetration. A modified IEEE-13 distribution feeder was built, considering the functionality of each scaled module and its generator-load under the Universidad del Norte laboratory conditions. An experimental methodology was used to compare the results obtained in the actual scaled model with the results of specialised programme simulations. The conclusions describe the amount of wind energy that can be injected into an electrical system that includes conventional power generation, while maintaining operation in compliance with the current regulatory framework.

#### RESUMEN



<sup>1</sup>BSc. in Electrician Engineering, Universidad del Norte, Colombia. Current position: Proinges SAS, Colombia. E-mail: eeguis@uninorte.edu.co

<sup>2</sup>BSc. in Electrician Engineering, Universidad del Norte, Colombia. Current position: Zona Franca Celsia, Colombia. E-mail: kmpadilla@uninorte.edu.co

<sup>3</sup>BSc. in Electrician Engineering, Universidad del Norte, Colombia. E-mail: llopeza@uninorte.edu.co

<sup>4</sup>BSc. in Electrician Engineering, Universidad Técnica de Georgia, Georgia. MSc. Universidad Técnica de Georgia, Georgia. Current position: Universidad del Norte, Colombia. E-mail: jsoto@uninorte.edu.co

<sup>5</sup>BSc. in Electrician Engineering, Universidad del Norte, Colombia. MSc. Universidad del Norte, Colombia. Current position: Universidad del Norte, Colombia. E-mail: rcastillo@uninorte.edu.co

<sup>6</sup>BSc. in Electronic Engineering, Universidad del Norte, Colombia. PhD. Instituto de Tecnología de Georgia, Georgia. Current position: Universidad del Norte, Colombia. E-mail: mpardo@uninorte.edu.co

<sup>7</sup>BSc. in Electrician Engineering, Universidad Tecnológica de Pereira, Colombia. PhD. Universidad Federal de Rio Grande del Sur, Brasil. Current position: Universidad del Norte, Colombia. E-mail: chenaoo@uninorte.edu.co

<sup>8</sup>BSc. in Electrician Engineering, Instituto Tecnológico de Santo Domingo, República Dominicana. MSc. Politécnica de Madrid, España. Current position: Instituto Tecnológico de Santo Domingo, República Dominicana. E-mail: elvin.jimenez@intec.edu.co

<sup>9</sup>BSc. in Electrician Engineering, Universidad del Norte, Colombia. PhD. Politécnica de Madrid, España. Current position: Universidad del Norte, Colombia. E-mail: inoliver@uninorte.edu.co

**Palabras clave:**

Generación Distribuida  
Pérdidas Eléctricas  
Eficiencia Energética  
IEEE-13  
Energías Renovables  
Energía Eólica

En este artículo se presentan los resultados del análisis de los estudios de la operación de un alimentador de distribución IEEE-13 modificado, que fue construido a escala en el laboratorio en la Universidad del Norte. En este artículo, se muestran los casos de los regímenes de operación del IEEE-13 modificado, ante los diferentes niveles de penetración de energía eólica. Este alimentador de distribución IEEE-13 modificado se construyó teniendo en cuenta que cada uno de los módulos escalados y su generador-carga funcionarán en las condiciones particulares del laboratorio de la Universidad del Norte. Se utilizó una metodología experimental que, para la comparación de los resultados obtenidos en el modelo real escalado, con los resultados de las simulaciones en programas especializados. Se pudo definir la cantidad de energía eólica que se puede inyectar a un sistema eléctrico con generación de energía convencional, de modo que pueda mantener su funcionamiento, no sólo respetando las condiciones técnicas, sino también bajo el estricto cumplimiento de un marco regulatorio.

## 1. Introduction

The installed electrical generation capacity in Colombia's Non-Interconnected Zones (Spanish acronym ZNI) is 99.9% diesel generation. Access to electricity in the ZNI is scarce and service is expensive; the real cost of electricity corresponds to twice the average cost per kWh of that in the National Interconnected System, with the aggravating circumstance that the area only receives service during half of the day's hours [1]. For this reason, plans have targeted a contribution of 30% of the installed capacity of electricity generation from non-conventional energy sources in the ZNI by 2020. This is supported by law 1715, passed in 2014, which promotes the use of non-conventional sources of energy, mainly in the ZNI, with the purpose of strengthening the national energy supply within a sustainable economic framework [2].

High levels of renewable energy penetration in conventional distribution systems present a new challenge for the normal operation of the system [3]. Several authors have centred their work on integration of distribution systems with emerging renewable technologies, including distributed wind generation [4-6]. The distributed wind generation alters the normal operation of the system due to the resource's inherent intermittency and its limited capacity to deliver reactive power to the network [7]. In Méndez et al. [8], the performance losses of the distribution system due to the high penetration of distributed generation in the network were evaluated. The authors present an approach to calculate annualised losses in the system due to varying levels of penetration and concentration of wind energy in the system.

Moustafa et al. [4] propose a methodology for the optimal integration of distributed generation of wind resources and energy storage systems. In the discussion, the intermittency of wind power generation systems was

shown to affect the operating costs of the distribution system for the companies providing the service. The increase in costs occurs when the penetration of wind energy in the distribution system increases. Therefore, the proposal aimed at optimally locating energy storage systems that mitigate the intermittency of distributed wind generation, subject to technical constraints.

Ahmadi and Ghasemi [9] propose a method to determine the maximum penetration level of wind farms based on synchronous turbines and doubly fed induction turbines. Considering the random nature of wind speed, the authors performed a transient stability analysis to determine the maximum penetration level of the wind farms. The results suggested that a high penetration of wind generators reduces of the general inertia of the system. To remedy this, a methodology was proposed based on a unit commitment with restrictions due to the wind farms.

In [10], Liew and Strbac studied the embedded wind generation connection in a rural-type distribution system. Rural distribution systems have the particular characteristics of large coverage distances and scattered loads. These particularities present a challenge for maximising the benefits of wind generation and transforming conventional distribution systems into active distribution systems. The authors presented and evaluated three insertion strategies throughout the research work: wind generation during periods of low demand, wind generation with compensation of reactive power, and wind generation with control via tap changing transformers.

Other research focuses on system variables, such as power quality, operating costs and the risks associated with the integration of distributed wind generation. In Mahela et al. [11], the power quality is studied in distribution networks with high wind penetration. Zubo

et al. [12] present a distribution market proposal for the integration of networks with high wind and solar penetration. In Chang et al. [13], analysis was undertaken of the risks associated with high wind penetration for the transmission systems and the existing generators in the network.

The energy strategic area at the Universidad del Norte has developed a microgrid in order to recreate real operating scenarios similar to the networks of the ZNI [14]. The microgrid has generation modules that emulate non-conventional energy sources. Contributions of the wind profiles can be modelled and simulated, enabling different operating conditions to be studied.

The microgrid and its generation modules allow evaluation of variables including energy efficiency, increase in non-conventional renewable energy use, reduction of greenhouse gas emissions, increase in security of supply and minimisation of electrical losses.

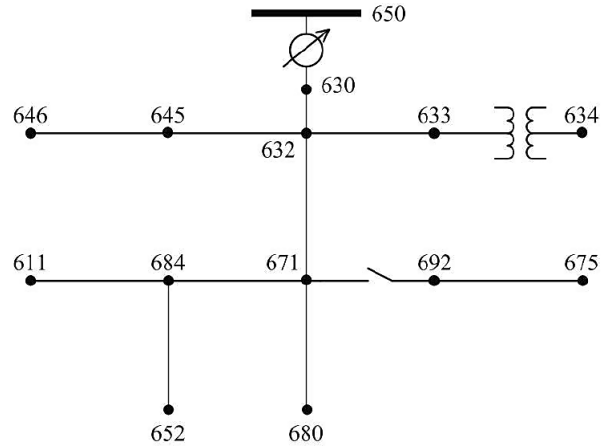
The designed microgrid is scaled to the voltage level of 220 V. The microgrid is composed of the local distribution network and the emulators based on the IEEE-13 standard. In addition, a model was developed with specialised software to evaluate the network under different operating scenarios, including: a steady-state study of the microgrid connected to, and isolated from the Local Distribution Network (LDN), as well as a study of the isolated dynamic state of the network.

## 2. Basic design of the microgrid

### 2.1. Topology selection

The distribution network model was selected according to the IEEE-13 test feeder, and adapted for laboratory work, as shown in Figure 1.

Figure 1: Modified IEEE 13 one-line diagram.

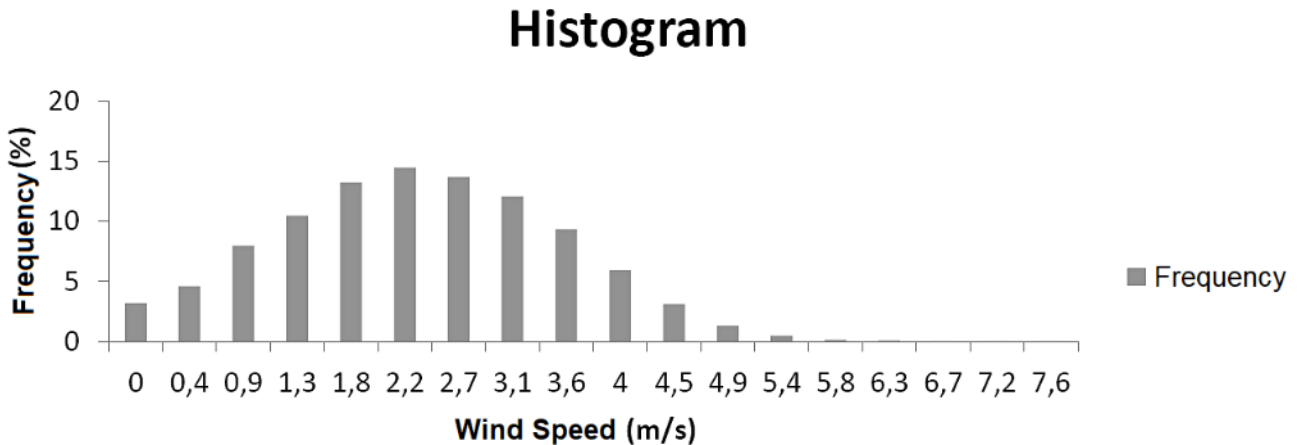


Source: own.

### 2.2. Wind speed study

The wind speed measurements enabled a statistical profile to be elaborated. With historical data, the measures of central tendency and dispersion for the data set were calculated during the recorded months. In this manner, it was possible to visualise the distribution of the wind frequency, as shown in Figure 2. Eighteen wind speeds were identified. The wind speed with the highest frequency was 2.2 m/s.

Figure 2: Wind speed histogram.



Source: own.

### 2.3. Characteristics of the wind turbine and diesel generator

The ENAIR wind turbine was selected for its efficiency, design and capacity to generate electricity at considerably low wind speeds [15]. This wind turbine has a starting speed of 1.8 m/s and an efficient generation range of 2 to 60 m/s, with a nominal power of 1900 W. The machine operates according to IEC 61400 class IA [16]. In addition, it has a controller for battery charging and connection to the local network.

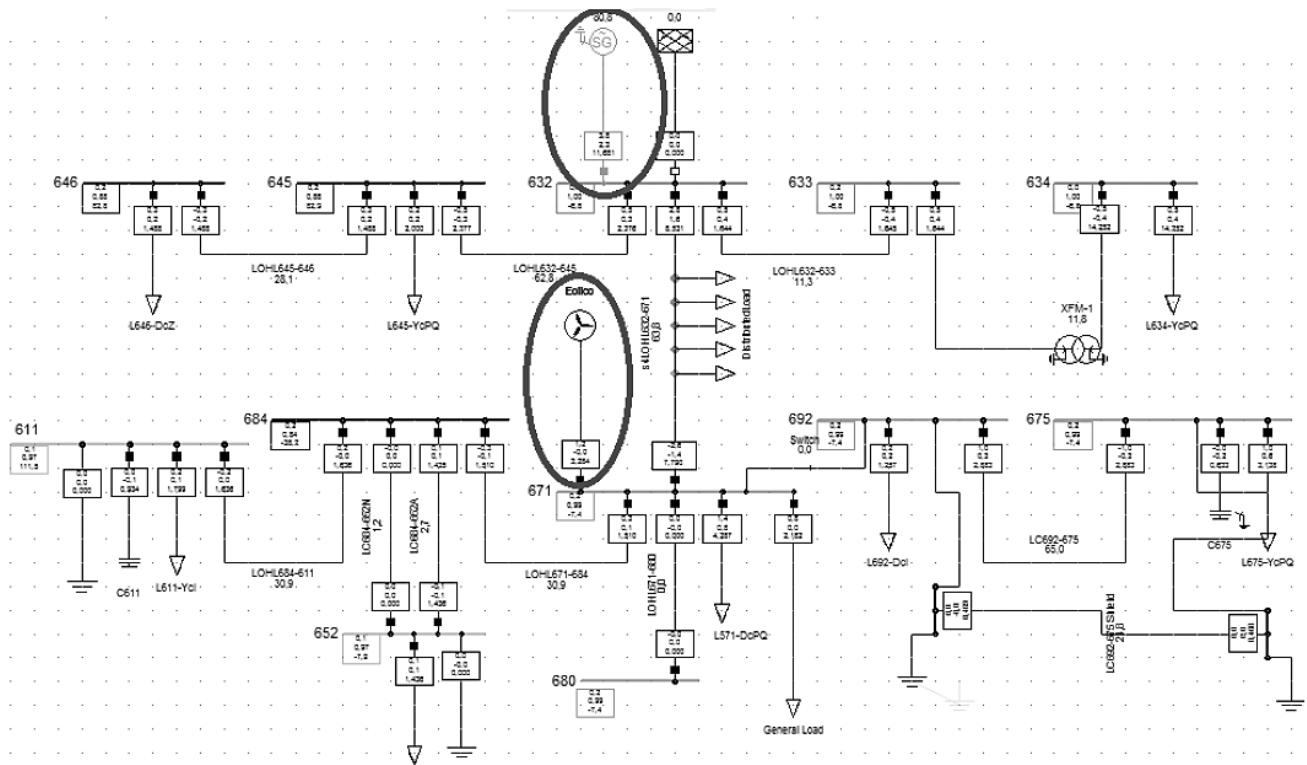
The wind turbines and the diesel plant were characterised according to the modified model of the IEEE-13 standard. Correspondingly, the plant was modelled with the characteristics of the synchronous generators of the Laboratory of Electrical Machines (LEM) at the Universidad del Norte. For the wind

turbines, the factor and power curve of the machine were specified, as well as the nominal voltage and power. Figure 3 presents the simulated system using specialised software, with connections to the wind turbines and the diesel plant.

### 3. Wind energy generation

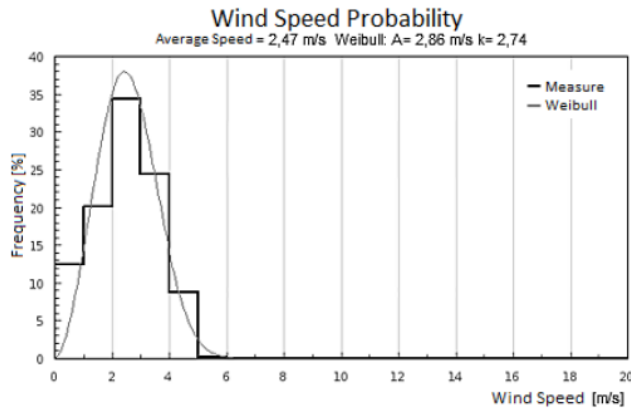
The wind potential was determined with a Weibull distribution, using the known environmental characteristics of the site and technical characteristics of the selected wind turbine, as shown in Figure 4. The wind turbine has a sweep radius of 1.9 m, which allowed it to reach an accumulated power of 1155.45 W during the seven months of data collection (Table 1). Based on the wind speed analysis, the estimated energy per month that the wind turbine could generate is shown in Table 2.

Figure 3: Software model of IEEE-13 Test feeder.



Source: own.

Figure 4: Wind speed probability distribution.



Source: own.

Table 1: Wind turbine power ENAIR E30 Pro.

Month	Wind Power (W)
October	28,227
November	23,779
December	148,892
January	234,286
February	247,380
March	317,574
April	155,318
Total	1155,45

Source: own.

Table 2: Wind energy per month.

Month	Average energy 24h per month (Wh)	Energy peak (Wh)	Hour
October	524,56	48,14	1:00 - 1:55 pm
November	509,62	53,12	1:00 - 1:55 pm
December	2693,3	169,3	4:00 - 4:55 pm
January	5	2	
	4125,9	243,1	12:00 - 12:55 pm
February	3	9	
	4097,7	261,4	3:00 - 3:55 pm
March	1	5	
	5039,7	296,3	2:00 - 2:55 pm
April	6	1	
	2623,6	224,9	3:00 - 3:55 pm
	3	3	

Source: own.

#### 4. Design of experiments

For the experimental design, four case studies were established (Table 3) based on three criteria, and taking the location of non-conventional generation sources in the microgrid into account. The first criterion is that the monophasic and biphasic nodes were not considered as possible connection points. As a second criterion, node 632 was not considered for the inclusion of renewable sources, since it is the microgrid's connection point to the network. Additionally, node 632 is the connection point for the diesel plant for the isolated case. Finally, the third criterion considered the distance between the renewable source and the demand locations. The wind turbines were located in the nodes with highest demand, in order to minimise losses and voltage drops.

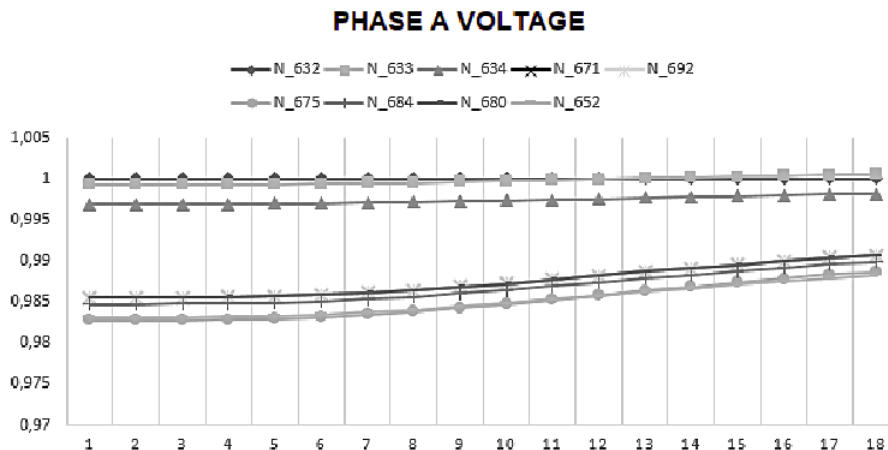
Table 3: Case studies.

Case 1 -	Distributed generation concentrated in node 680, a node without generation or initial demand.
Case 2 -	Generation distributed in nodes 633, 671 and 675, three-phase nodes close to demand.
Case 3 -	Distributed centralised generation in node 671, the central node in the network. In addition, the node has the largest centralised demand in the network (33.3% of total active power demand).
Case 4 -	Distributed generation centralised in node 675, the node with the second highest demand (24.3% of the total active demand of the network).

Source: own.

Based on the previous observations of the wind response to transient voltage tests. However, the models tested in transient simulations, it was concluded that the existing models would provide an acceptable were not suitable for the small signal stability test [17].

Figure 5: Voltage phase A – Case 2.



Source: own.

## 5. Analysis and results

### 5.1. Steady-state study: connected to, and isolated from the distribution network

In this section, we present the simulations of the steady-state system connected to, and isolated from the LDN, wherein two methods were used for data analysis. The first method consisted of analysing the system's response variables in each case study. The second method selected the case study with the best response to wind generation integration in the network. The results presented below were obtained by the first method.

#### 5.1.1. Voltage analysis

The voltages of phase A, shown in Figure 5, are within the range established by the Comisión de Regulación de Energía y Gas CREG 024 de 2005 [18] for the injection of renewable sources into the network. The voltages of phase B presented a negative response to the increase in power injection from the wind turbines. Phase B exhibited the same tendency as the other phases, with an increase in voltage in the nodes near the power injection point. However, the increase in voltage at B resulted in relatively significant overvoltage at nodes 671, 675, 692 and 680.

The voltages of phase C demonstrated a consistent response among the different case studies; the behavioural trend was an increase in the voltage at the nodes that presented the worst regulation values (nodes 671, 692, 675, 680, 684, 652 and 611). Contrastingly, the

nodes exhibiting the best regulation values (645, 646, 633 and 634) maintained almost constant voltage values despite the changes in active wind power injected into the network.

#### 5.1.2. Line loadability analysis

**Case 1:** The increase in wind generation resulted in a decrease in current in line 632-671. At the same time, there was an increase in current in line 671-680, because all the wind generation was concentrated in node 680. Despite this, no overloads were generated in this case study.

**Case 2:** The distribution of wind generation in the network caused a more significant response in the system. The loadability of lines 632-671, 632-633 and 692-675 was reduced to the point where the wind turbine generation exceeded the local demand and thus began to provide power to the rest of the system. However, it should be clarified that in this case study there were no operating condition violations due to overloads in the lines.

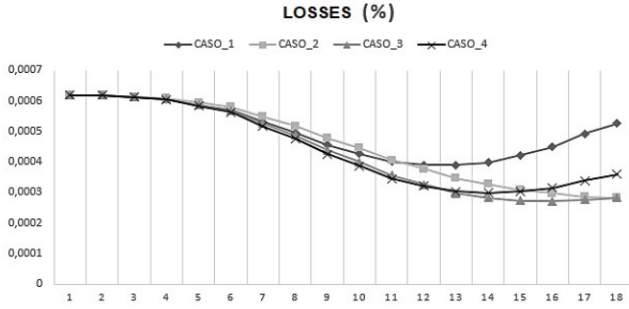
**Case 3:** This case did not provide a greater contribution than decreasing the flow transported by line 632-671. No overloads on the lines were generated.

**Case 4:** Line 632-671 showed a decrease in current, while the current in line 692-675 also decreased because the demand located in node 675 began to be met by wind turbines. With a high penetration, the current of line 692-671 increased its loadability, but with an inverse flow to that presented before. In this case, there was an overload of 120 % of the line's nominal value.

5.1.3. Power loss analysis

The response of the system to the inclusion of renewable energy appeared as a decrease in the total losses of the system (within the wind ranges studied). Figure 6 shows that cases 3 and 4 achieved the lowest loss curve values.

Figure 6: Power losses of the system after the inclusion of renewable energy.



Source: own.

During the study method development, a statistical analysis of each of the system’s response variables was carried out. First, we studied the voltages, by calculating the Root Mean Square Error (RMSE) for each case. In this analysis, the errors or differences between the voltages of every node and the ideal voltage (1 p.u.) throughout the iterative process of the DIGSILENT Programming Language (DPL) were calculated. Next, equation (1) was used to calculate the RMSE of every node.

$$RMSE = \sqrt{\frac{1}{n} \sum_{j=1}^n |V_{ref} - V_j|^2} \tag{1}$$

Where:

$n$ : Number of iterations (18 iterations).

$V_j$ : Node voltage at iteration  $j$ .

$V_{ref}$ : Reference value of the voltage (1 p.u.).

Thus, in 67% of the phase A nodes, case study 4 presented the smallest deviations with reference to the voltage of 1 p.u. In the second case study, the lowest RMSE values were exhibited in the remaining nodes, as shown in Table 4. The voltages of phase B demonstrate the same response. The lowest RMSE values (67% of the nodes) in phase B were found in the second case, as shown in Table 5.

Table 6 shows the phase C voltage values, among which 50% of the nodes displayed lower RMSE values in the fourth case study. In contrast, 20% of the remaining nodes had a better response in the second case study and only 10% obtained the best RMSE values in the first case study.

In summary, the voltages in the nodes of the microgrid presented the best response to the inclusion of wind sources in case 4, where the lowest RMSE values were obtained for 62% of the voltages analysed.

Subsequently, an analysis of the loadability of the microgrid lines was carried out. Table 7 shows the overload that occurred in case 4, due to the overload generated in line 675-692.

Additionally, Table 7 shows the average total losses expressed as a percentage of power obtained. Significantly, the third case study does not exceed the loadability restrictions of the line conductors, while also having the second-best voltage response and the lowest losses. Therefore, the dynamic study will analyse the centralised wind generation in node 671.

Table 4: RMSE Voltage Phase A.

RMSE Voltage Phase A				
NODE	CASE 1	CASE 2	CASE 3	CASE 4
N_632	0	0	0	0
N_633	0,0732	0,0498	0,0732	0,0731
N_634	0,3115	0,2648	0,3115	0,3114
N_671	1,1895	1,2643	1,1866	1,1853
N_692	1,1895	1,2643	1,1866	1,1853
N_675	1,4630	1,5150	1,4599	1,3890
N_684	1,2672	1,3429	1,2642	1,2629
N_680	1,0952	1,2642	1,1866	1,1853
N_652	1,4261	1,5035	1,4230	1,4216

Source: own.

**Table 5:** RMSE Voltage Phase B.

<b>RMSE Voltage Phase B</b>				
<b>NODE</b>	<b>CASE 1</b>	<b>CASE 2</b>	<b>CASE 3</b>	<b>CASE 4</b>
<b>N_632</b>	0	0	0	0
<b>N_645</b>	0,3375	0,3375	0,3375	0,3375
<b>N_646</b>	0,4112	0,4112	0,4112	0,4112
<b>N_633</b>	0,1056	0,0706	0,1057	0,1058
<b>N_634</b>	0,2939	0,2463	0,2940	0,2941
<b>N_671</b>	0,2785	0,2463	0,2837	0,2813
<b>N_692</b>	0,2785	0,2463	0,2837	0,2813
<b>N_675</b>	0,4264	0,4244	0,4312	0,5179
<b>N_680</b>	0,3342	0,2463	0,2837	0,2813

Source: own.

**Table 6:** RMSE Voltage Phase C.

<b>RMSE Voltage Phase C</b>				
<b>NODE</b>	<b>CASE 1</b>	<b>CASE 2</b>	<b>CASE 3</b>	<b>CASE 4</b>
<b>N_632</b>	0	0	0	0
<b>N_645</b>	0,0015	0,0015	0,0015	0,0015
<b>N_646</b>	0,0024	0,0024	0,0024	0,0024
<b>N_633</b>	0,0017	0,0012	0,0017	0,0017
<b>N_634</b>	0,0039	0,0033	0,0039	0,0039
<b>N_671</b>	0,0172	0,0179	0,0172	0,0172
<b>N_692</b>	0,0172	0,0179	0,0172	0,0172
<b>N_675</b>	0,0184	0,0190	0,0184	0,0179
<b>N_684</b>	0,0182	0,0189	0,0181	0,0181
<b>N_611</b>	0,0190	0,0197	0,0189	0,0189
<b>N_680</b>	0,0162	0,0179	0,0172	0,0172

Source: own.

**Table 7:** Maximum loadability and average power losses.

	<b>LOADABILITY</b>	<b>AVERAGE POWER LOSSES</b>
	(%)	(%)
<b>CASE 1</b>	69,189	0,000499
<b>CASE 2</b>	70,447	0,000459
<b>CASE 3</b>	70,447	0,000435
<b>CASE 4</b>	120,467	0,000444

Source: own.

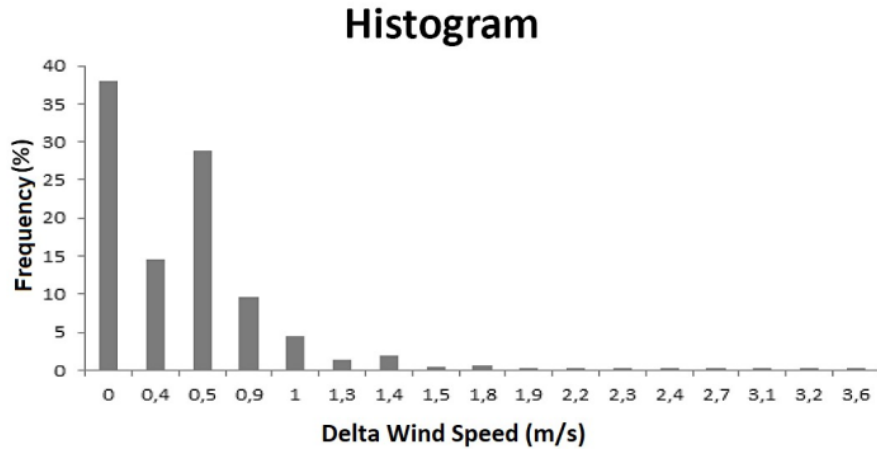
The results presented so far correspond to the scenario where the microgrid operates connected to the local distribution network. Likewise, steady-state studies were carried out for an isolated case. The difference

between the response of the system operating in isolation from, and connected to the LDN is not significant.

## 5.2. Dynamic study of the isolated distribution network

RMS simulations were carried out in which the frequency and voltage response of the system was analysed under the fluctuations of wind and demand. First, the dynamic study of the system was carried out under wind speed fluctuations. In Figure 7, the histogram of the wind speed changes between two continuous measurements is shown. Additionally, Figure 7 indicates that the greatest wind speed variation recorded between two continuous measurements was 3.6 m/s.

**Figure 7:** Histogram of variations in recorded wind speeds.



Source: own.

Initially, the response of the system to the variation in power generated by three wind turbines was simulated. Therefore, the network was subjected to a power swap of 2520 W in 5 minutes (8.4 W/s). Based on the above considerations, the following results were obtained (Figure 8).

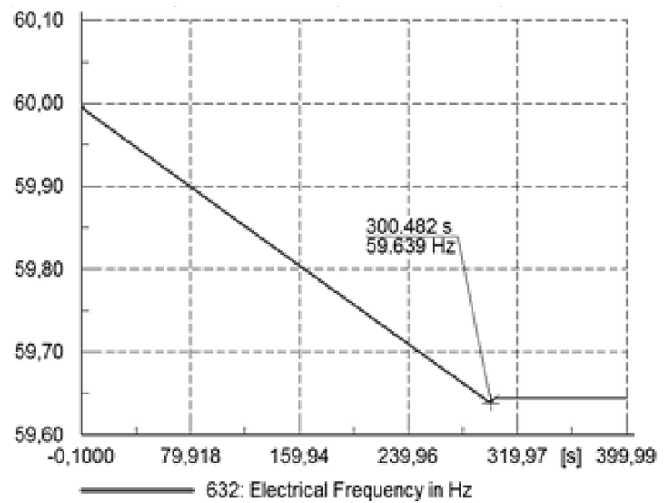
When the network is governed based on the change of power generated by the wind turbines, a progressive imbalance between generation and demand originates. In this case, following the loading event, the frequency was 59,468 Hz.

Moreover, the inertia of the system plus that of the diesel generator could not maintain acceptable operating conditions in the system when faced with the variation in the power produced by the three wind turbines. For this reason, the same analysis was carried out with two wind turbines. Figure 8 shows the frequency results of the two-turbine event studied.

Subsequently, given that the conditions for frequency regulation were again not reached, the system analysis was carried out with a single wind turbine, with the response shown in Figure 8.

Consequently, the largest instantaneous change under which the system can maintain the frequency ranges accepted by the distribution system design standard [19] is 934 W. The results show that power changes exceeding 22% of the system demand cause unacceptable changes in frequency. The aforementioned data are shown in Table 8.

**Figure 8:** Frequency response during the critical change with 2 wind turbines.



Source: own.

**Table 8:** Frequency response to sudden changes in demand.

Total Demand (W)	Power demand	Power demand	Frequency (Hz)
	change (%)	change (W)	
4243	10%	424,3	59,91
	20%	848,6	59,82
	22%	933,46	59,8

Source: own.

## 6. Conclusions and recommendations

Initially, historical wind data analysis was carried out at the Universidad del Norte, in which low wind speeds were found in comparison to those required to support the proposed microgrid. The power and energy generated by the wind turbines were minimal in relation to the requirements of the microgrid. Wind potential corresponds to less than 10% of the total demand of the system. The greatest potential recorded was in the month of March, with a total of 317.5 W, when the power demanded by the system is 4228 W. The highest wind generation peak of 296.31 Wh also occurred during the month of March. When considering the losses that occur when incorporating renewable energy into the system, it can be concluded that these are minimised by having a wind contribution. In the system studied, the resulting variations were within the range of  $\pm 0.005$  p.u.

Among the different case studies analysed, the best connection point for the wind generators was found to be node 671, because it presented the lowest percentages of losses, no overloads in the lines and, in addition, node voltages that remained within the range established by legislation. In the same way, by directly injecting wind power into the network from wind turbines and studying the frequency response of the system, it was concluded that the number of wind turbines that can be implemented is limited to one. Otherwise, the conditions of stability would be violated due to the fluctuations of power injected by the wind turbines. Finally, a sudden change in demand of up to 934 W may occur so that the frequency does not exceed the regulatory ranges, which represents a change in demand equal to 22%.

## 7. Acknowledgements

This research was supported by the Strategic Energy Area of Universidad del Norte. We appreciate the knowledge and resources provided that helped a lot in the research.

## References

- [1] J. Flórez, D. Tobón and G. Castillo, “¿Ha sido efectiva la promoción de soluciones energéticas en las zonas no interconectadas (ZNI) en Colombia?: un análisis de la estructura institucional,” Cuadernos de administración, vol. 22, no. 38, 2009, pp. 219–245.
- [2] Congreso de Colombia, “Ley 1715. Mayo 2014,” 2014. [Online]. Available at: [http://www.secretariassenado.gov.co/senado/basedoc/ley\\_1715\\_2014.html](http://www.secretariassenado.gov.co/senado/basedoc/ley_1715_2014.html)
- [3] G. Pepermans, J. Driesen, D. Haeseldonckx, R. Belmans and W. D’haeseleer, “Distributed generation: Definition, benefits and issues,” Energy Policy, vol. 33, no. 6, 2005, pp. 787–798. <https://doi.org/10.1016/j.enpol.2003.10.004>
- [4] Y. M. Atwa and E. F. El-Saadany, “Optimal allocation of ESS in distribution systems with a high penetration of wind energy,” IEEE Trans. Power Syst., vol. 25, no. 4, 2010, pp. 1815–1822. <https://doi.org/10.1109/TPWRS.2010.2045663>
- [5] M. R. Baghayipour, A. Hajizadeh, A. Shahirinia and Z. Chen, “Dynamic placement analysis of wind power generation units in distribution power systems,” Energies, vol. 11, no. 9, 2018, pp. 1–16. <https://doi.org/10.3390/en11092326>
- [6] K. Maki, “Effect of wind power based distributed generation on protection of distribution network,” Eighth IEEE International Conference on Developments in Power System Protection, 2005, pp. 327–330. <https://doi.org/10.1049/cp:20040129>
- [7] T. R. Ayodele, A. Jimoh, J. L. Munda and A. J. Tehile, “Challenges of Grid Integration of Wind Power on Power System Grid Integrity: A Review,” Int. J. Renew. Energy Res., vol. 2, no. 4, 2012, pp. 618–626.
- [8] V. Mendez, J. Rivier and T. Gomez, “Assessment of Energy Distribution Losses for Increasing Penetration of Distributed Generation,” IEEE Trans. Power Syst., vol. 21, no. 2, 2006, pp. 533–540. <https://doi.org/10.1109/TPWRS.2006.873115>
- [9] H. Ahmadi and H. Ghasemi, “Maximum penetration level of wind generation considering power system security limits,” IET Gener. Transm. Distrib., vol. 6, no. 11, 2012, pp. 1164–1170.
- [10] S. N. Liew and G. Strbac, “Maximising penetration of wind generation in existing distribution networks,” IEEE Proc. - Gener. Transm. Distrib., vol. 149, no. 3, 2002, pp. 256–262.
- [11] O. P. Mahela, P. Prajapati and S. Ali, “Investigation of Power Quality Events in Distribution Network with Wind Energy Penetration,” IEEE Int. Students’ Conf. Electr. Electron. Comput. Sci. SCEECS, 2018, pp. 1–5. <https://doi.org/10.1109/SCEECS.2018.8546945>
- [12] R. H. A. Zubo, G. Mokryani and R. Abd-Alhameed, “Optimal operation of distribution networks with high penetration of wind and solar power within a joint active and reactive distribution market

- environment,” *Appl. Energy*, vol. 220, 2018, pp. 713–722. <https://doi.org/10.1016/j.apenergy.2018.02.016>
- [13] Y. Chang et al., “Risk Assessment of Generation and Transmission Systems Considering Wind Power Penetration,” *Int. Conf. Power Syst. Technol. POWERCON*, 2018, pp. 1169–1176. <https://doi.org/10.1109/POWERCON.2018.8601737>
- [14] P. De la Hoz, A. Silva, R. Castillo-sierra, I. Oliveros, M. Pardo and E. Jimenez, “UniGRID: Photovoltaic Study Case for the Universidad del Norte Renewable Energies,” *15th International Conference on Electrical Engineering, Computing Science and Automatic Control (CCE)*, 2018, pp. 1–6. <https://doi.org/10.1109/ICEEE.2018.8533985>
- [15] ENAIR, “Aerogenerador ENAIR E30 PRO Ficha Técnica,” [Online]. Available at: <https://www.enair.es/es/Aerogeneradores/E30PRO>
- [16] IEC, “IEC International Standard 61400-1,” 2008, pp. 1–9. [Online]. Available at: [https://webstore.iec.ch/preview/info\\_iec61400-1%7Bed3.0%7Den.pdf](https://webstore.iec.ch/preview/info_iec61400-1%7Bed3.0%7Den.pdf)
- [17] J. Conto, “Grid challenges on high penetration levels of wind power,” *IEEE Power Energy Soc. Gen. Meet.*, 2012, pp. 1–3. <https://doi.org/10.1109/PESGM.2012.6344717>
- [18] Comisión de Regulación de Energía y Gas - CREG, “Resolución No. 024 de 2005,” 2005. [Online]. Available at: [http://www.creg.gov.co/html/Ncompila/htdocs/Documentos/Energia/docs/resolucion\\_creg\\_0024\\_2005.htm](http://www.creg.gov.co/html/Ncompila/htdocs/Documentos/Energia/docs/resolucion_creg_0024_2005.htm)
- [19] Empresa Electrificadora de Santander ESSA, “Norma Técnica ESSA”, Normas para cálculo y diseño de sistemas de distribución,” 2004. [Online]. Available at: <https://www.essa.com.co/site/Portals/14/Docs/Norma%20tecnica/Norma%20T%C3%A9cnica%20ESSA.pdf>